

# MATHEMATICAL MODELLING OF RESIN INFILTRATION IN RESIN TRANSFER MOULDING (RTM)

C.Lekakou and M.G.Bader  
Department of Materials Science and Engineering  
University of Surrey  
Guildford, Surrey GU2 5XH

## Abstract

A mathematical model is proposed to describe the macro- and micro-infiltration in Resin Transfer Moulding. Macro- and micro-properties include permeabilities and capillary pressures. Parametric computational studies are carried out to study the flow of a model Newtonian fluid through woven cloths where the following parameters are varied: fibre volume fraction, macro properties of reinforcement and global flowrate. When the pore Reynolds number is sufficiently high, inertia effects are expected to be significant and numerical procedures are suggested for the determination of global permeability and inertia coefficient in the cases of rectilinear and radial flow.

## 1. INTRODUCTION

Impregnation of the fibre reinforcement by the polymer matrix is a key factor affecting ply consolidation and void elimination in the processing of polymer composites. In the case of the reinforcement consisting of fibre bundles, two distinct types of impregnation are available: macro- and micro-impregnation. Macro-impregnation controls mould filling and elimination of large-scale dry spots. Micro-impregnation concerns resin flow between individual fibres, inside fibre bundles, and affects micro-porosity and the quality of fibre/matrix interface. The two phenomena are closely related since there is a mass balance between macro- and micro- resin flow. The two types of pores are associated to the macro- and micro- permeability of the fibre reinforcement and the wetting properties at the resin/fibre interface. Other parameters affecting both types of impregnation are resin rheology, applied mechanical pressure and/or vacuum and filling length in the mould.

A large group of published papers focus on microscopic studies of void formation in composites manufacturing [see Mahale et al (1) and Nowak and Chun (2) amongst others]. Void formation is related to resin impregnation and more specifically to viscous flow and wetting properties of resin related to the reinforcement. With regards to the modelling of impregnation, Darcy's law has generally been used to describe the infiltration of viscous resin through a porous medium. However, several experimental studies illustrated that the flow behaviour of Newtonian fluids in

both saturated and unsaturated reinforcements deviated from Darcy's law with the permeability being a function of porosity, superficial velocity of permeating fluid and pressure drop [3-6]. At high flowrates and pressures, inertia effects are as important as viscous effects and, hence, Cai [7-8] suggested that Darcy's law is replaced by Ergun's equation. However, the dependence of the permeability on the superficial velocity was observed even at low superficial velocities [Chan et al (3) and Lekakou et al (4)] where inertia effects were negligible. Chan et al (3) speculated that the observed increase in permeability with flowrate could be due to a preferential channelling of the liquid through the large pores (macro-flow) rather than through the micro-pores within fibre tows (micro-flow).

In flow visualisation studies Molnar et al (9) and Patel et al (10) observed that at a low flowrate micro-flow was leading whereas at a high flowrate macro-flow was leading. This illustrated the need for developing a mathematical model for the macro- and micro-infiltration. Chan and Morgan [11-12] constructed a model for macro- and micro-infiltration in bi-directional non-woven fabrics. Darcy's law was employed for both macro- and micro-flow but capillary pressures and wetting effects were not taken into account. Micro-flow inside the tows was considered only in the radial direction until each tow was fully impregnated.

The scope of the current study is to carry out a theoretical analysis of infiltration of reinforcement in RTM for the two main types of flow used in in-plane permeability measurements: (a) rectilinear flow from a side gate and (b) radial flow from a central gate. Radial flow is used frequently in the measurement of the global in-plane permeability as it is easy to determine simultaneously the components of in-plane permeability from the axes of the elliptical flow front. A model has been constructed to describe the combined phenomena of macro- and micro-infiltration where separate permeabilities are used for the macro- and micro-flow and capillary pressures are taken into account. Computational parametric studies follow in which the effects of the following variables are investigated: porosity, permeabilities, capillary pressures and global flowrate. Ergun's equation is applied in the case of high injection pressures and it is demonstrated how to determine the empirical constants for the two main types of flow.

## 2. MATHEMATICAL MODEL OF MACRO- AND MICRO-INFILTRATION

Darcy's law has been employed to describe the relation between flowrate and pressure drop, at low flowrates and injection pressures, in both macro- and micro-impregnation where the impregnating fluid was considered to be Newtonian. Since only viscous effects are considered in Darcy's law, this analysis is applicable to very low pore Reynolds numbers,  $Re_p$ , where

$$Re_p = \frac{\rho U D_e}{\mu} \quad (1)$$

and  $D_e$  is the equivalent pore diameter.

The case of radial global flow from a central gate has been considered:

*Macro-flow:*

*Radial flow*

*Rectilinear flow*

$$Q_{ma} = \frac{2\pi h K_{ma}}{\mu} \frac{(\Delta P + P_{ma}^c)}{\log(R_f/R_o)} \qquad Q_{ma} = \frac{Ah K_{ma}}{\mu} \frac{(\Delta P + P_{ma}^c)}{\Delta x} \qquad (2)$$

*Micro-flow<sub>II</sub>:* 
$$Q_{mi, II} = \frac{\Delta N_{tow} \pi r_{tow}^2 K_{mi, II}}{\mu} \frac{(\Delta P + P_{mi, II}^c)}{\Delta L_{tow}} \qquad (3)$$

*Micro-flow<sub>I</sub>:* 
$$Q_{mi, I} = \frac{2\pi \Delta L_{tow}^{tot} r_{mi, I} K_{mi, I}}{\mu} \frac{(\Delta P + P_{mi, I}^c)}{\log(r_{tow}/r_{tow, I})} \qquad (4)$$

The micro-permeabilities have been determined from the Carman-Kozeny equation where the Kozeny parameter  $k_{o,II}$  has been taken as 0.5 and  $k_{o,I}$  as 10 [13-15]. The capillary pressures were calculated according to the relation suggested by Ahn et al (16).

Regarding the modelling of the combination of macro- and micro-infiltration three modes of flow have been considered (see Figure 1). In mode I the fibre tows have not been fully impregnated in the radial direction; the flow then is considered as channelled mainly into the macro-pores and from there the fluid simultaneously impregnates the fibre tows in the radial direction. In mode II the fibre tows are considered as fully impregnated in the radial direction; the flow then is considered as being split between macro-impregnation and micro-impregnation along the fibre direction. In mode III the fibre tows are considered as fully impregnated in the radial direction and the flow front is ahead inside the tows; the flow is then modelled as a combination of micro-impregnation along the fibre direction and simultaneous transverse flow from the tows into the micropores.

The problem is solved numerically by employing the finite difference technique. At every time step every numerical position along the main macro-flow path in the mould behind the flow front is considered. At the flow front it is examined if impregnation will lead inside the macro-pores (mode I) or inside the tows (mode III). Similarly behind the flow front, it is examined whether

the tows are fully impregnated (mode II) or have not been yet fully impregnated (mode I). Then at every radial position the flowrate is split between macro- and micro- flowrate. The pressure at the junction of split is considered as  $P_i$ , the pressure at the numerical position  $R_i$  or  $x_i$ . However, the pressure at the flow front interface is different in each outlet of the junction, being  $P_{ma}^c$  in the macro-flow,  $P_{mi,II}^c$  in the micro-flow parallel to the fibres and  $P_{mi,I}^c$  in the radial micro-flow. This generates different total pressure differences in equations (2)-(4). The three types of permeability in these equations are also different. Macro- and micro-flowrates are estimated following a trial-and-error procedure (17).

### 3. MATHEMATICAL MODEL INCLUDING THE INERTIA EFFECTS

Momentum transport for the general case of flow through a porous medium, including both inertia and viscous terms, is described by the following relation in rectilinear coordinates:

$$a \rho U^2 + \frac{\mu}{K} U = \frac{\Delta P}{\Delta x} \quad (5)$$

where the first and second terms on the right hand side represent the inertia and viscous terms, respectively. Relation (5) can be easily considered as the outcome of a combination of Ergun's and Carman-Kozeny equations.  $K$  denotes a global permeability and  $a$  denotes an inertia coefficient to be determined from experimental data. Relation (5) can be used at high injection pressures where capillary effects may be ignored.

In order to determine the empirical constants  $a$  and  $K$  in rectilinear flow experiments, relation (5) is rewritten as follows:

$$\frac{Ah\Delta P}{\mu Q \Delta x} = \frac{1}{K} + a \frac{\rho Q}{\mu Ah} \quad (6)$$

Under constant injection pressure experiments  $Q$  is recorded as a function of filling length  $\Delta x$ , whereas under constant flowrate experiments  $\Delta P$  is recorded as a function of  $\Delta x$ .

The equivalent relation for radial flow under constant flowrate is as follows:

$$\frac{\Delta P}{\mu Q \ln(R_f/R_o)} = \frac{1}{2\pi hK} + a \frac{\rho (1/R_o - 1/R_f) Q}{4\pi h^2 \mu \ln(R_f/R_o)} \quad (7)$$

## 4. RESULTS AND DISCUSSION

### 4a. PARAMETRIC STUDIES OF MACRO- AND MICRO-INFILTRATION

A series of computational parametric studies were carried out concerning the in-plane infiltration of five layers of a woven cloth, Y0212 from Courtaulds Advanced Materials, by silicone oil of  $\mu = 0.140$  Pas. The cloth was a plain weave glass fabric of a density of  $0.546 \text{ kg/m}^2$ , thickness  $0.48 \text{ mm}$ , containing  $6.7 \text{ ends/cm}$  and  $6.3 \text{ picks/cm}$  (used in the in-plane permeability measurements of Lekakou et al (4)). First the micro- and macro- impregnation times were compared in rectilinear flow under different constant injection pressures for a mould filling length of  $0.3 \text{ m}$ . At low injection pressures, due to relatively long filling times, micro-impregnation could be considered to occur instantaneously: for example  $t_{mi}/t_{filling} \sim 1 \times 10^{-3}$ . At high injection pressures, filling occurs in short times which are comparable to micro-impregnation times as Figure 2 illustrates. The driving factors for micro-impregnation are the capillary and local mechanical pressures. Since the local mechanical pressure decreases as the fluid moves away from the gate, the micro-impregnation time increases.

In the next set of parametric studies, in which the layers of cloth were compressed to different fibre volume fractions, changes were taken into account at macro-level, i.e. macro-porosity and average size of macro-pores, while bundle dimensions and micro-porosity were assumed to remain the same. The following micro-properties were calculated:

$$\begin{array}{lll} \varepsilon_{mi} = 0.42 & K_{mi,\Pi} = 2.6 \times 10^{-12} \text{ m}^2 & K_{mi,I} = 1.3 \times 10^{-13} \text{ m}^2 \\ & P_{mi,\Pi}^c = 11720 \text{ Pa} & P_{mi,I}^c = 5860 \text{ Pa} \end{array}$$

In the parametric studies, the overall fibre volume fraction was varied from  $0.3$  to  $0.58$  resulting in the macro-porosity changing from  $0.48$  to  $0.034$  respectively. This resulted in large changes in the macro-properties,  $K_{ma}$  and  $P_{ma}^c$ , as is illustrated in Figure 3. At low  $V_f$  the macro-permeability is much higher than the micro-permeabilities whereas the macro-capillary pressure is much lower than the micro-capillary pressures. However, at high  $V_f$  the bundles come so close together that macro-properties approach micro-properties.

Table I: Permeabilities at various flowrates:

$Q1 = 6.76 \times 10^{-7} \text{ m}^3/\text{sec}$ ,  $Q2 = 2 \times Q1$ ,  $Q3 = 4 \times Q1$ ,  $Q4 = 8 \times Q1$ .

$V_f$	K2/K1	K3/K2	K4/K3
0.30	1.29	1.11	1.05
0.40	1.06	1.03	1.02
0.50	1.02	1.01	1.00
0.58	1.00	1.00	1.00

Computer simulations were then carried out to evaluate global permeabilities in radial flow at constant flowrate. A first set of overall permeabilities,  $K_1$ , was calculated for all the range of  $V_f$  at an infiltration flowrate  $Q_1 = 6.76 \times 10^{-7} \text{ m}^3/\text{sec}$ . Then the infiltration flowrate was increased and new sets of permeabilities  $K_i$  were calculated for the whole range of  $V_f$  corresponding to  $Q_i$ . Table I displays the ratios  $K_i/K_j$  for varying  $Q_i/Q_j$  and different  $V_f$ 's. At low  $V_f$  macro-flow is important. Low flowrates are generated from low applied mechanical pressures,  $\Delta P$ . At low  $\Delta P$  the micro-capillary pressures are important and produce micro-flowrates which cannot be neglected. As a result the macro-flowrate is reduced and this reduces the overall permeability which is calculated on the basis of  $\Delta P$ . As  $Q$  increases  $\Delta P$  also increases, capillary effects become less important and the flowrate is channelled towards the largest permeability, i.e. the macro-pores. The flow front then moves quickly as macro-flow first and this raises the permeability. As  $Q$  is raised further in the parametric studies the capillary effects become negligible and the flow is channelled primarily as macro-flow leading to constant  $K$ . On the other hand, as  $V_f$  is increased the macro-permeability is reduced. So, the effects of flow channelling into the macro-pores are less important and  $K$  changes less with  $Q$ . At  $V_f = 0.58$  macro- and micro-impregnation become almost identical and no change of permeability is calculated when the flowrate is varied.

#### 4b. STUDIES OF INERTIA EFFECTS

Inertia effects are present at relatively high injection pressures which are not usually employed in permeability measurements. A search of appropriate data in the literature yielded Trevino et al's study (6) in which a non-linear relation between pressure and superficial velocity was reported and injection pressures reached  $8 \times 10^5 \text{ Pa}$ . In that study there was no data of fibre or pore size and, hence, it was not possible to estimate the macro-flow Reynolds number. However, if relation (5) could be applied to Trevino et al's data, a linear relationship should exist between the variable groups  $\Delta P/U$  and  $U$ . As Figure 4 displays, the data could fit a linear relationship with a negative value for the inertia coefficient  $a$ , which is not acceptable. Therefore, the non-linear relation between injection pressure and superficial velocity in Trevino et al's data cannot be attributed to the presence of inertia terms. Figure 5 displays some data from the study of Lekakou et al (4) where the estimated macro-pore Reynolds number is 0.07. According to this data a small degree of inertia might be present at this  $Re_p$ , although there are no sufficient points in the graph for a reliable evaluation of the inertia coefficient,  $a$ .

#### 5. CONCLUSIONS

A mathematical model was suggested for macro- and micro-impregnation in the processing of polymer composites, including Darcy's and capillary effects. It was demonstrated that micro-impregnation times increase as the resin front moves away from the inlet port due to the corresponding decrease of local mechanical pressure. A series of computational parametric studies were performed for a range of fibre volume fractions, where macro- and micro-properties were calculated in each case. As the impregnation flowrate was increased from a low flowrate of  $6.76 \times 10^{-7} \text{ m}^3/\text{sec}$  the overall permeability initially increased in agreement with



previous experimental studies [3-4] due to the fact that micro-capillary effects become less important and flow is channelled into the macro-pores. Above a certain flowrate capillary effects become negligible and as a result the overall permeability remained constant. At high fibre contents the overall permeability also remained constant due to reduced differences between macro- and micro-flow.

It was demonstrated that inertia effects are usually negligible under RTM conditions. The value of pore Reynolds number should be a good indication for the presence of inertia effects, and, if present numerical procedures have been suggested for the determination of global permeability and inertia coefficient from experimental data in the cases of rectilinear and radial flow.

#### REFERENCES

1. Mahale A.D., Prud'homme R.K. and Rebenfeld L., Pol.Eng.Sci 32(5) (1992) 319.
2. Nowak T. and Chun J.-H., Composites Manufacturing 3(4) (1992) 259.
3. Chan A.W., Larive D.E. and Morgan R.J., J.of Composite Materials 27(10) (1993) 996.
4. Lekakou C., Johari M.A.K., Norman D. and Bader M.G., Composites Part A 27A (1996) 401.
5. Martin G.Q. and Son J.S., Proc. ASM/ESD 2nd Conf. on Advanced Composites, ASM International, Materials Park OH, 1986.
6. Trevino L., Rupel K., Young W.B., Liou M.J. and Lee L.J., Polymer Composites 12(1), 1991, 20.
7. Cai Z., J. of Advanced Materials, October 1993, 58.
8. Cai Z., J. of Composite Materials 29(2), 1995, 257.
9. Molnar J.A., Trevino L. and Lee L.J., Polymer Composites 10 (1989) 414.
10. Patel N., Rohatgi V. and James Lee L., Pol.Eng.Sci. 35(10) (1995) 837.
11. Chan A.W. and Morgan R.J., Polymer Composites 14(4) (1993) 335.
12. Chan A.W. and Morgan R.J., SAMPE Quaterly October (1992) 45.
13. Williams J.G., Morris C.E.M. and Ennis B.C., Pol.Eng.Sci. 14(6) (1974) 413.
14. Gutowski T.G., Cai Z., Bauer S., Boucher D., Kingery J. and Wineman S., J. of Composite Materials 21 (1987) 650.
15. Lam R.C. and Kardos J.L., Proc. Amer. Soc. Comps., 3rd Techn. Conf. Seattle WA (1988) 3.
16. Ahn K.J., Seferis J.C. and Berg J.C., Polymer Composites 12 (1991) 146.
17. Lekakou C. 'Simulation of flow, reaction and heat transfer in Reaction Injection Moulding', PhD Thesis, Imperial College (London), 1987.

#### ACKNOWLEDGMENTS

The authors would like to thank Mr David Norman for his help in the drawings.

## LIST OF SYMBOLS

$A$  = cross-sectional area ( $m^2$ )  
 $a$  = inertia coefficient  
 $D_e$  = equivalent pore diameter (m)  
 $\Delta L_{tow}$  = length of individual tow being impregnated in parallel flow in numerical control volume (m)  
 $\Delta L_{tow}^{tot}$  = total length of tows in numerical control volume (m)  
 $\Delta N_{tow}$  = no of tows in numerical control volume  
 $\Delta P$  = mechanical pressure difference (Pa)  
 $\varepsilon$  = porosity =  $(1 - V_f)$   
 $h$  = thickness of compressed sample (m)  
 $K$  = permeability ( $m^2$ )  
 $k_o$  = Kozeny parameter  
 $L$  = total filling length (m)  
 $\mu$  = viscosity (Pa s)  
 $P$  = pressure (Pa)

$P^c$  = capillary pressure (Pa)  
 $Q$  = flowrate ( $m^3/sec$ )  
 $R_f$  = radial position at flow front (m)  
 $R_o$  = radius of gate (m)  
 $r_{tow}$  = radius of tow (m)  
 $r_{tow,f}$  = non-impregnated radius of tow (m)  
 $\rho$  = density ( $kg/m^3$ )  
 $U$  = superficial velocity (m/sec)  
 $V_f$  = fibre volume fraction

### Subscripts

$ma$  = macro  
 $mi$  = micro  
 $\parallel$  = parallel to fibres  
 $\perp$  = normal to fibres

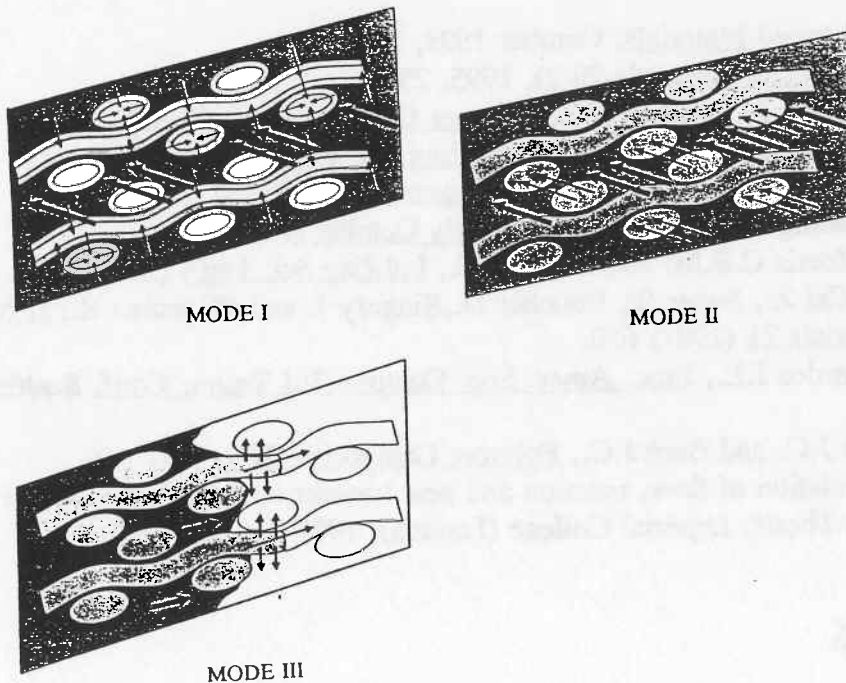


**Figure 1:** The three modes of the impregnation model for woven cloths.



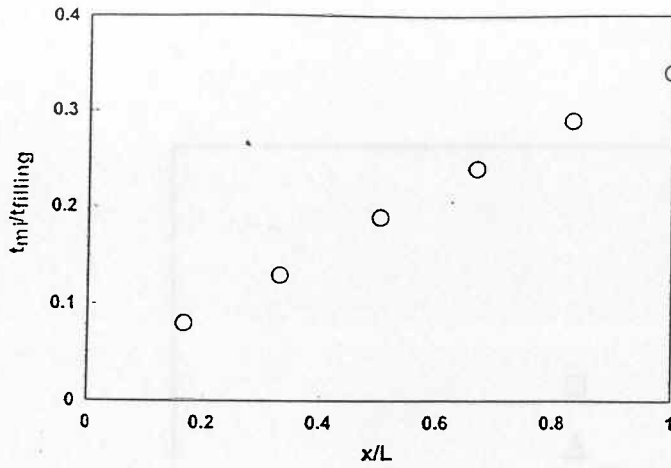


**Figure 2:** A comparison between micro-impregnation and filling times in rectilinear flow under constant injection pressure of  $8 \times 10^5$  Pa.

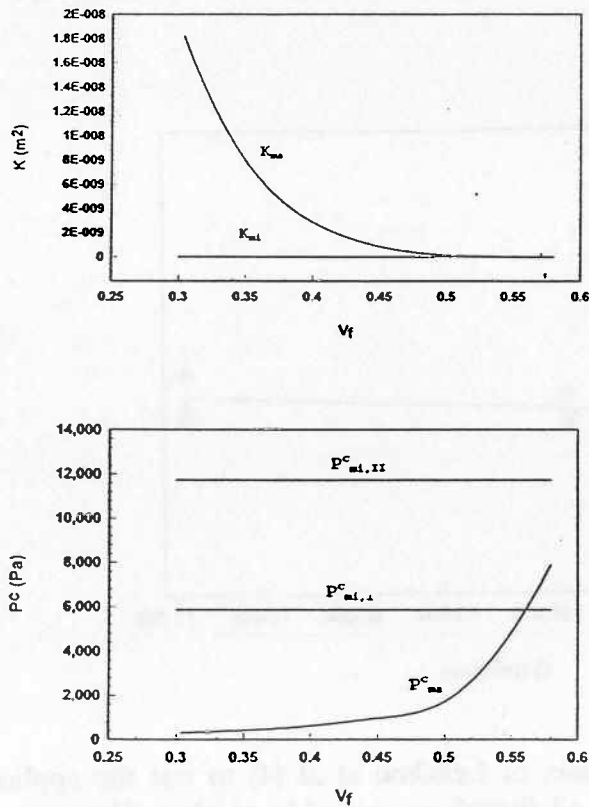


**Figure 3:** Macro- and micro-properties (permeability and capillary pressure) as functions of global fibre volume fraction.

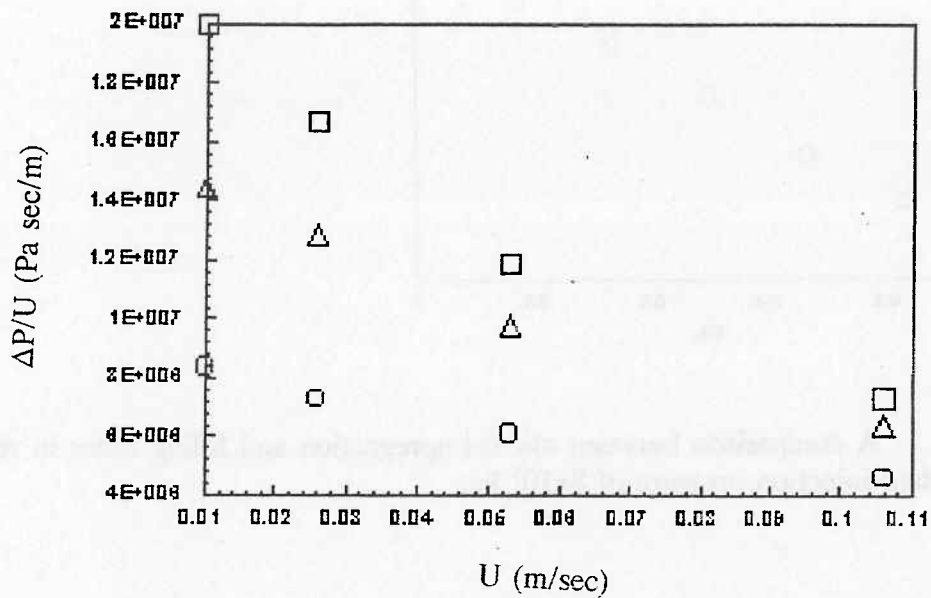


**Figure 4:** Graphs of experimental data of Trevino et al (6) to test the applicability of relation (5); rectilinear flow of DOP oil through a random glass fibre mat.  $\circ$  :  $V_f=0.23$ ;  $\Delta$  :  $V_f=0.34$ ;  $\square$  :  $V_f=0.46$ .

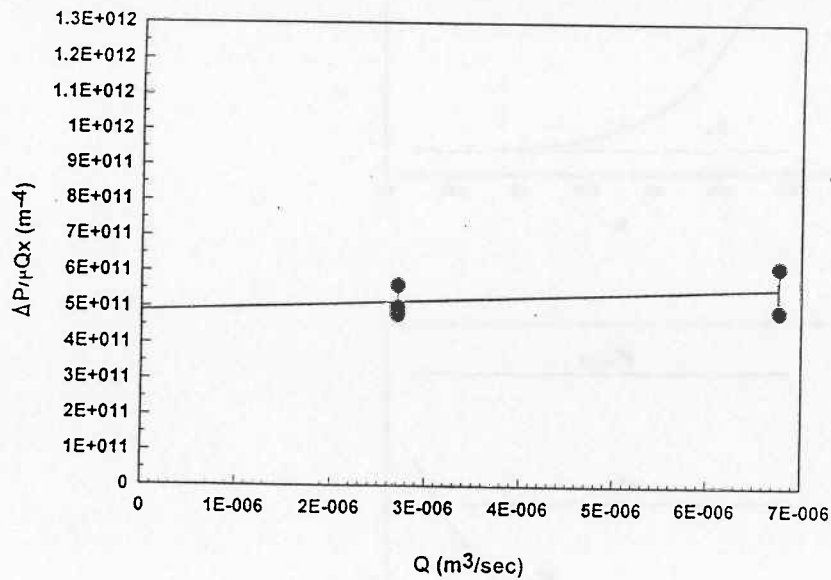


**Figure 5:** A graph of experimental data of Lekakou et al (4) to test the applicability of relation (5); rectilinear flow of silicone oil through an assembly of glass fibre woven cloths.  $Re_p = 0.07$ .